J. Microbiol. Biotechnol. (2015), 25(2), 162–173
http://dx.doi.org/10.4014/jmb.1410.10067

jmb

Effect of Changes in the Composition of Cellular Fatty Acids on Membrane Fluidity of *Rhodobacter sphaeroides*

Eui-Jin Kim and Jeong K. Lee*

Department of Life Science, Sogang University, Seoul 121-742, Republic of Korea

Received: October 30, 2014
Revised: November 17, 2014
Accepted: November 24, 2014

First published online
November 24, 2014

**Corresponding author*
Phone: +82-2-705-8459;
Fax: +82-2-704-3601;
E-mail: jgklee@sogang.ac.kr

Supplementary data for this paper are available on-line only at http://jmb.or.kr.

pISSN 1017-7825, eISSN 1738-8872

The cellular fatty acid composition is important for metabolic plasticity in *Rhodobacter sphaeroides*. We explored the effects of changing the cellular ratio of unsaturated fatty acids (UFAs) to saturated fatty acids (SFAs) in *R. sphaeroides* by overexpressing several key fatty acid biosynthetic enzymes through the use of expression plasmid pRK415. Bacteria containing the plasmid pRKfabI$_1$ with the *fabI$_1$* gene that encodes enoyl-acyl carrier protein (ACP) reductase showed a reduction in the cellular UFA to SFA ratio from 4 (80% UFA) to 2 (65% UFA) and had decreased membrane fluidity and reduced cell growth. Additionally, the ratio of UFA to SFA of the chromatophore vesicles from pRKfabI$_1$-containing cells was similarly lowered, and the cell had decreased levels of light-harvesting complexes, but no change in intracytoplasmic membrane (ICM) content or photosynthetic (PS) gene expression. Both inhibition of enoyl-ACP reductase with diazaborine and addition of exogenous UFA restored membrane fluidity, cell growth, and the UFA to SFA ratio to wild-type levels in this strain. *R. sphaeroides* containing the pRKfabB plasmid with the *fabB* gene that encodes the enzyme β-ketoacyl-ACP synthase I exhibited an increased UFA to SFA ratio from 4 (80% UFA) to 9 (90% UFA), but showed no change in membrane fluidity or growth rate relative to control cells. Thus, membrane fluidity in *R. sphaeroides* remains fairly unchanged when membrane UFA levels are between 80% and 90%, whereas membrane fluidity, cell growth, and cellular composition are affected when UFA levels are below 80%.

Keywords: *Rhodobacter sphaeroides*, enoyl-ACP reductase, fatty acids, β-ketoacyl-ACP synthase I, membrane fluidity

Introduction

In bacteria, fatty acids are synthesized by discrete monofunctional enzymes, in what is known as a type II system [55]. In bacterial fatty acid synthesis, the enzyme β-ketoacyl-ACP synthase III (FabH) catalyzes an initial decarboxylative condensation between acetyl-CoA and malonyl-ACP to yield acetoacetyl-ACP [25]. This β-ketoacyl-ACP is subsequently reduced, dehydrated, and reduced again by the serial reactions of a β-ketoacyl-ACP reductase (FabG), a β-hydroxyl-ACP dehydratase (FabA or FabZ), and a *trans*-Δ^2-enoyl-ACP reductase (FabI) [55]. Condensation of the acyl moiety with malonyl-ACP in successive elongation cycles is performed by another enzyme, β-ketoacyl-ACP synthase I (FabB), while the last condensation is mediated by β-ketoacyl ACP synthase II (FabF) [19]. Chain elongation is generally known to stop when the cycles produce a palmitic (C16) or a stearic (C18) saturated acid. FabI is a key enzyme in the type II fatty acid synthase system because it catalyzes the last reduction at each cyclic elongation [21], and its activity appears to affect overall cellular fatty acid composition [18]. Moreover, it has been known as an appropriate target for antibacterial agents such as triclosan, isoniazid, and diazaborine [5, 7, 24, 32, 45].

For the synthesis of an unsaturated fatty acids (UFA), double bonds can be introduced into the growing acyl chain by FabA, which is a bifunctional enzyme that has both dehydratase and isomerase activities. The β-hydroxydecanoyl-ACP is dehydrated by either FabA or an

isoenzyme, FabZ, to form *trans*-Δ^2-decenoyl-ACP, which can be further isomerized by FabA into its *cis*-Δ^3-decenoyl-ACP [37]. Four more cyclic elongations then lead to the formation of the unsaturated *cis*-vaccenic acid (18:1(Δ^{11})).

Alternatively, UFAs may be generated by a desaturase that introduces a double bond into a pre-existing fatty acid attached to ACP, glycolipid, and coenzyme A (CoA) [1, 41, 48]. The desaturases may be present in the cytosol as acyl-ACP desaturase or bound to the membrane as acyl lipid desaturase and acyl-CoA desaturase. Because desaturases are mixed-function oxidases, their activities depend on the presence of O_2. In a few bacteria, such as *Bacillus subtilis*, *Pseudomonas aeruginosa*, and *Synechocystis* spp., membrane fluidity is regulated by controlling the expression of desaturase genes in response to changes in temperature and or the presence of exogenous fatty acids [10, 46, 56]. However, it is not currently known exactly how bacteria regulate membrane fluidity in response to environmental changes.

Alterations in the composition of fatty acids may affect membrane fluidity, which is known to significantly alter the cellular metabolic homeostasis [40, 49]. A decrease in the fluidity of thylakoid membranes results in the inhibition of photosynthetic (PS) electron transport in cyanobacteria and plants, highlighting the significance of membrane fluidity for PS efficiency [23]. Moreover, lipid unsaturation is essential for protection of PS complexes from environmental stresses, such as high light, high salt, and high and low temperatures [33].

The cellular fatty acid composition would be also important for metabolic plasticity in the purple non-sulfur photosynthetic bacterium *Rhodobacter sphaeroides*, which has been used as a model organism to study photosynthesis and its related gene expression. The bacterium forms photosynthetic chromatophores in the intracytoplasmic membrane (ICM). The entire PS machinery, including the reaction center (RC) complex, B875 light-harvesting (LH) complex, and the most peripheral B800-850 LH complex, are exclusively localized within the ICM. O_2-dependent regulation for the expression of the apoproteins of the PS spectral complexes and the biosynthetic enzymes for bacteriochlorophyll (Bch) *a* and carotenoids have previously been elucidated [34, 43].

Membrane fluidity affects the function of many membrane proteins that work within the lipid bilayer [36]. It has been suggested that appropriate lipid-protein interactions are important for the proper functioning of the PS complexes of *R. sphaeroides* [8, 13, 26]. To our knowledge, however, the effect of changes in fatty acid composition on membrane fluidity in *R. sphaeroides* has not been examined. Here, we explored the effects of changing the cellular ratio of UFA to saturated fatty acids (SFA) in *R. sphaeroides* by overexpressing several key fatty acid biosynthetic enzymes. We found that the ratio of UFA to SFA of *R. sphaeroides*, which is normally approximately 4 (80% UFA), was reduced by half (65% UFA, ratio of 2) when *fabI*$_1$ expression was elevated, whereas the ratio was increased more than 2-fold (90% UFA, ratio of 9) when *fabB* expression was elevated. Bacteria with a lowered UFA content of 65% had significantly lower membrane fluidity and reduced cell growth, but the formation of ICM under photoheterotrophic conditions was not changed. The UFA content in chromatophore vesicles and the quantity of light-harvesting complexes were also reduced with the elevated expression of *fabI*$_1$. However, PS gene expression was not altered under this condition. Cells overexpressing *fabI*$_1$ exhibited cellular UFA content, membrane fluidity, and growth rates similar to control cells when FabI$_1$ was inhibited with diazaborine and when exogenous UFAs were added to the growth medium. The UFA to SFA ratio more than doubled (90% UFA) through the elevated expression of *fabB*, but membrane fluidity was not changed. Thus, the membrane fluidity of *R. sphaeroides* remains unchanged when relative UFA levels in the membrane stay within a range of approximately 80% to 90%, but membrane fluidity appears to be considerable decreased when UFA levels are below 80%.

Materials and Methods

Bacterial Strains and Growth Conditions

R. sphaeroides 2.4.1 was used as the wild-type strain and grown at 28°C in Sistrom's succinate-based (Sis) minimal medium [51] as described previously [15]. Cells were grown aerobically by vigorous shaking (250 rpm) on a gyratory shaker or by sparging (more than 100 ml/min gas flow per 100 ml culture) with a defined gas mixture of 30% O_2, 1% CO_2, and 69% N_2. Cells were grown photoheterotrophically (15 W/m^2) in completely filled screw-cap tubes or by sparging with a gas mixture of 2% CO_2 and 98% N_2. Alternatively, cells were grown anaerobically in the dark with 75 mM dimethyl sulfoxide (DMSO). Cell growth was monitored in Klett unit (KU) using a Klett-Summerson colorimeter (Manostat) equipped with a KS-66 filter. *E. coli* was grown at 37°C in Luria-Bertani medium. Antibiotics for *R. sphaeroides* and *E. coli* cultures were added at concentrations as indicated previously [28].

Construction of Plasmids

The DNA fragment containing *fabI*$_1$ [30] was cloned from the cosmid pUI8123 [16], whereas *fabA*, *fabB*, and *fabI*$_2$ were obtained through PCR from genomic DNA of *R. sphaeroides*. The 1.5 kb *Xho*I/*Sma*I DNA containing *fabI*$_1$, the 1.1 kb *Nsi*I/*Nru*I DNA

containing *fabA*, the 1.9 kb *Sma*I/*Sac*I DNA containing *fabB*, and the 1.3 kb *Bgl*II/*Bam*HI DNA containing *fabI*$_2$ were cloned into pBS (Stratagene) and then subsequently ligated into pRK415 [27] to generate pRKfabI$_1$, pRKfabA, pRKfabB, and pRKfabI$_2$, respectively. All the open reading frames were cloned in the same orientation as the *lac* promoter of pRK415.

The transcriptional fusion construct *puhA-lacZ* was prepared as follows; a 1.0 kb *Eco*RI/*Xba*I DNA extending from 1,005 bp upstream from the initiation codon of *puhA* to its 7th codon was PCR amplified with the forward primer (5′-**G<u>A</u>A T<u>T</u>C** ACA TGA CCC AGA CGG C-3′, where the *Eco*RI site is in bold and the mutated sequences are underlined unless indicated otherwise) and reverse primer (5′-**TC<u>T</u> A<u>G</u>A** AGC AGT CAC ACC AAC C-3′, where the *Xba*I site is in bold), and then transcriptionally fused to *lacZ* [50] on IncQ plasmid pLV106 [31] to generate pHZ300.

The pLV106 [31] derivatives, pUI1830 [20], pCF200 [31], and pHZ300, which carry the transcriptional fusion constructs of *puf-lacZ*, *puc-lacZ*, and *puhA-lacZ*, respectively, were mobilized from *E. coli* S17-1 into *R. sphaeroides* harboring pRKfabI$_1$, pRKfabB, or pRK415 through conjugation as described previously [11].

Determination of PS Spectral Complexes

The cell-free extracts of *R. sphaeroides* grown exponentially under photoheterotrophic conditions were prepared as described previously [53]. The amount of B800-850 complex was calculated from the spectrophotometric profile by using $A_{849\text{-}900}$ with an extinction coefficient (ε) of 96 mM^{-1} cm^{-1}, whereas the amount of B875 complex was determined using $A_{878\text{-}820}$ with ε of 73 mM^{-1} cm^{-1} [39].

Purification of ACP

R. sphaeroides acpP coding for ACP was expressed in *E. coli* BL21 (DE3) pLysS containing pRSET-ACP [30]. The hexahistidine-ACP (H_6-ACP) was purified using a Ni^{2+}-NTA agarose column (Qiagen) as described previously [22]. The purified H_6-ACP was analyzed by SDS–PAGE containing Tricine as described previously [47]. Protein concentration was determined using a modified Lowry method [35] with bovine serum albumin as a standard.

Preparation of Crotonyl-ACP

Crotonyl-ACP was synthesized by thioesterification between the purified H_6-ACP and crotonic anhydride as described previously [24]. The level of crotonyl-ACP was determined using the Ellmann technique [17], and it was found that approximately 85% of ACP was acylated.

Purification of Chromatophore Vesicles

Cell-free extracts were suspended in 1 mM Tris-HCl (pH 7.5) containing 1 mM EDTA, and were fractionated for chromatophore vesicles by centrifugation at 96,000 ×*g* for 4 h on a linear sucrose gradient (5–35%) as described previously [54].

Enzyme Assays

Enoyl-ACP reductase activity was measured in a standard assay mixture containing 10 mM sodium phosphate buffer (pH 6.5), 150 μM crotonyl-ACP, 300 μM NADH, and an appropriate amount of cell extracts. The initial reaction rate was measured at 30°C through monitoring the decrease in A_{340} as a measure for NADH oxidation with concomitant reduction of crotonyl-ACP [24]. The specific activity was expressed as μmol·min^{-1}·mg $protein^{-1}$.

The β-galactosidase activities (Miller units) from *puf-lacZ*, *puc-lacZ*, and *puhA-lacZ* fusion constructs were determined as described previously [52].

Quantitative Analysis of Membrane Fatty Acids by Gas Chromatography

The fatty acid composition of membrane lipids was analyzed as described previously with minor modifications [6]. Total lipids were extracted from cells with 3.8 ml of chloroform/methanol/water (2:1:0.8, by volume), which were then mixed with 1 ml of 1 M KCl/0.2 M H_3PO_4, followed by centrifugation for the partitioning of lipids into the chloroform phase. The lipid extracts were concentrated by evaporation under a stream of N_2. A modified silicic acid column chromatographic method was used to eliminate free fatty acids from the lipid extracts as described previously [14]. Fatty acid methyl esters (FAMEs) were prepared after 1 h incubation of lipid extracts with 1 ml of 1 M methanolic-HCl at 79°C. Then, 1 ml of 1% (w/v) KCl was added, and the FAMEs were extracted with 1 ml of hexane. The resulting FAMEs were dried to a volume of 0.1 ml and then analyzed with gas chromatograph (GC-17A, Shimadzu), which was equipped with a capillary column (30 m × 0.25 mm; length × internal diameter) coated with polyethylene glycol (VB-WAX, VICI), and a flame ionization detector. For quantitative determination of fatty acids in membrane lipids, pentadecanoic acid (internal standard) and heptadecanoic acid methyl ester (external standard) were added to the samples before and after esterification, respectively. A FAME standard (37-component FAME; Supelco) was used to compare the retention times of the FAMEs. A *cis*-vaccenic acid (Sigma-Aldrich) was esterified and used as a control, because *cis*-vaccenic acid methyl ester was not included in the FAME standard.

Quantitative Analysis of Lipids by Gas Chromatographic Analysis of FAMEs

The compositions of the membrane lipids were determined as described previously [6]. The lipid extracts, which had been prepared as described above, were spotted onto activated silica thin-layer chromatography (TLC) plates (Si250; Baker). Two-dimensional TLC was performed with the first developing mixture of chloroform/methanol/water (65:25:4, by volume), followed by the second mixture of chloroform/acetone/methanol/acetic acid/water (50:20:10:10:5, by volume). Individual lipid spots were visualized with iodine vapor and scraped out to determine the levels of fatty acids as described above. The lipid composition of the cell was calculated as mole % of the fatty acids in each lipid. Two fatty acids were counted per molecule of lipids, except for cardiolipin, where four acyl chains were present per lipid.

Measurement of Fluorescence Anisotropy

Membrane fluidity was measured using a spectrofluorometer (QM-4; Photon Technology International) equipped with a temperature-controlled cuvette holder and two polarizers set in either a vertical or a horizontal position, as described previously [3]. Cells during exponential growth were harvested and suspended to an A_{600} of 0.4 in 50 mM Tris-HCl buffer (pH 7.0). Cell suspensions were incubated for 10 min with 4×10^{-6} M 1,6-diphenyl-1,3,5-hexatriene (DPH) in the dark, which is a lipophilic probe to determine the membrane dynamics. Fluorescence anisotropy was determined at 23°C, 28°C, and 33°C. Excitation and emission wavelengths were set at 358 nm and 428 nm, respectively. The samples were excited with vertically polarized light, and the vertical and horizontal emission intensities were recorded. Results were expressed as fluorescence anisotropy (A, unitless), which is defined as the ratio of polarized components to the total intensity by the equation $A = I_{II} - I_{\perp}/I_{II} + 2I_{\perp}$, where I_{II} and $I_{\perp}$ are the fluorescence intensities parallel and perpendicular to the direction of the excitation light beam, respectively. The background fluorescence of non-labeled samples was less than 2% of that of the labeled ones.

All the experiments were independently repeated three times; data shown are representative of one of three experiments or the average values with standard deviation (SD).

Results

Growth of *R. sphaeroides* Harboring pRKfabI$_1$ (Rs-fabI$_1$) was Reduced Relative to Control Cells.

R. sphaeroides contains two distinct enoyl-ACP reductases, FabI$_1$ and FabI$_2$. FabI$_1$ is a major enzyme in fatty acid biosynthesis and is indispensable for cell growth, whereas the biochemical role of FabI$_2$ has not been characterized [30]. Because changes in relative levels of SFA and UFA in *E. coli* have been observed through variation of the expressions of *fabI* and *fabB* [12, 21, 38], we asked whether the fatty acid composition of *R. sphaeroides* would vary when the dosage of the above-mentioned *fab* genes is increased. The DNA fragments of *fabI$_1$*, *fabA*, *fabB*, and *fabI$_2$* were cloned into the expression vector pRK415, and the resulting recombinant plasmids were mobilized into *R. sphaeroides*. Interestingly, the colony pigmentation of Rs-fabI$_1$ was lighter compared with control cells containing pRK415. The other recombinants showed the same colony pigmentation as control cells. The growth of Rs-fabI$_1$ was retarded under both aerobic (Fig. 1A) and anaerobic (Figs. 1B and 1C) conditions. Growth under photoheterotrophic conditions was the most severely affected (Fig. 1B). *R. sphaeroides* harboring pRKfabB (Rs-fabB) grew similarly to control cells (Fig. 1), and the same was true for cells harboring pRKfabA and pRKfabI$_2$ (data not shown, but similar to that observed with control cells of Fig. 1).

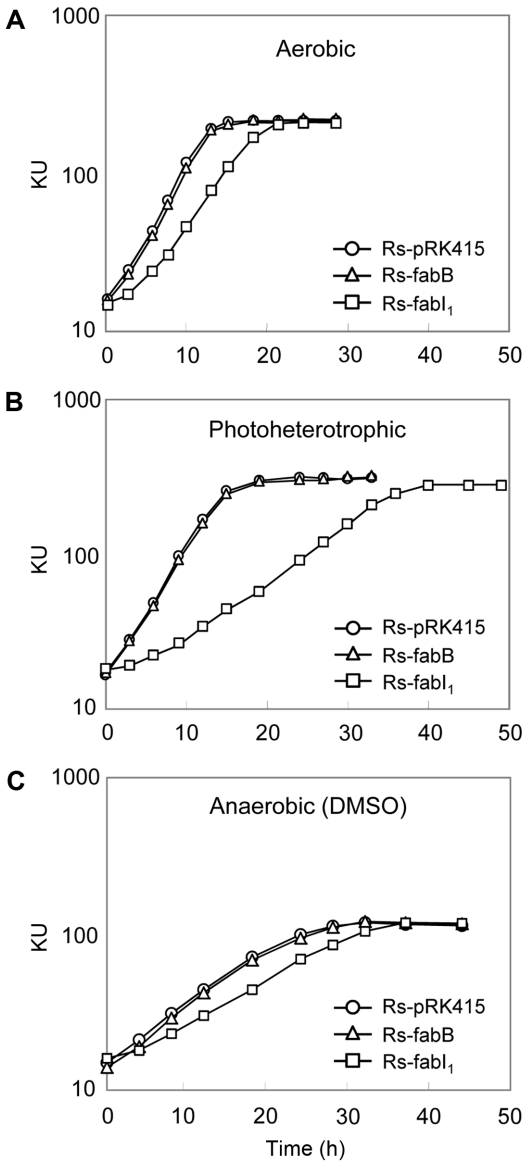

Fig. 1. Growth of *R. sphaeroides* harboring either pRKfabI$_1$ (Rs-fabI$_1$) or pRKfabB (Rs-fabB).

Rs-fabI$_1$ and Rs-fabB were grown under aerobic (**A**), photoheterotrophic (**B**), and anaerobic dark (with DMSO) (**C**) conditions. *R. sphaeroides* harboring pRK415 (Rs-pRK415) was included as a control. The experiments were independently repeated three times; data shown are representative of one of three experiments.

The Ratio of UFA to SFA was Reduced by Half in Rs-fabI$_1$, and was More than Doubled in Rs-fabB.

Because the photoheterotrophic growth of *R. sphaeroides*

Table 1. Fatty acid composition of membrane lipids of aerobically (O_2) and photoheterotrophically (PS) grown Rs-fabI$_1$, Rs-fabB, and Rs-pRK415.

Culture conditions	Strain	Composition of fatty acids (mole %)					UFA/SFA[a]
		C16	C16:1(Δ^9)	C18	C18:1(Δ^{11})	C19[b]	
O_2	Rs-pRK415	7.3 ± 0.6	1.5 ± 0.5	13.7 ± 2.0	75.3 ± 3.0	2.2 ± 0.4	3.76
	Rs-fabI$_1$	10.3 ± 0.5	0.5 ± 0.1	23.1 ± 2.0	62.7 ± 2.7	3.3 ± 0.5	1.99
	Rs-fabB	3.4 ± 0.5	1.7 ± 0.4	7.0 ± 1.3	86.1 ± 2.6	1.9 ± 0.3	8.63
PS	Rs-pRK415	4.9 ± 0.4	1.8 ± 1.0	14.1 ± 1.9	77.4 ± 0.6	1.8 ± 0.5	4.28
	Rs-fabI$_1$	10.0 ± 4.9	0.5 ± 0.1	24.1 ± 5.5	63.1 ± 9.3	2.2 ± 0.2	1.93
	Rs-fabB	2.9 ± 0.6	1.3 ± 0.2	6.5 ± 0.9	87.6 ± 1.2	1.6 ± 0.3	9.67

[a]The molar ratio of UFAs (C16:1(Δ^9), C18:1(Δ^{11}), and C19) to SFAs (C16 and C18).

[b]*cis*-11,12-Methyleneoctadecanoic acid was confirmed by gas chromatography-mass spectrometry analysis and by its absence from the lipid extracts of the *cfaS* mutant (data not shown).

was largely affected by the expression of pRKfabI$_1$, the composition of membrane fatty acids of these cells was determined (Table 1). The proportion of *cis*-vaccenic acid (C18:1(Δ^{11})), normally the most abundant UFA, decreased by approximately 15 mole % compared with control cells, whereas stearic acid (C18) and palmitic acid (C16) almost doubled (Table 1). On the other hand, the *cis*-vaccenic acid content in Rs-fabB increased by approximately 10 mole %, while the stearic acid and palmitic acid content decreased approximately by half (Table 1). Similar changes in fatty acid composition in the presence of pRKfabI$_1$ and pRKfabB were observed in aerobically grown cells (Table 1). Taken together, the ratio of UFA to SFA decreased by half in the presence of pRKfabI$_1$, but the ratio doubled in the presence of pRKfabB (Table 1). Neither pRKfabA nor pRKfabI$_2$ had any effect on the ratio of UFA to SFA (data not shown but similar to that observed in the control cells of Table 1). Thus, the growth rate of *R. sphaeroides* is attenuated when the UFA to SFA ratio is decreased from 4 (~80% UFA) to 2 (~65% UFA), but growth remains unaffected when the ratio is increased to 9 (~90% UFA).

Rs-fabI$_1$ had Decreased Levels of LH Complexes, but No Change in ICM Content or Photosynthetic Gene Expression

The presence of pRKfabB did not affect the levels of light-harvesting complexes (Fig. 2). However, the presence of pRKfabI$_1$ resulted in lower levels of LH complexes (Fig. 2), where the B875 complex decreased approximately by half, and the 800–850 complex decreased 4-fold compared with control cells. We measured transcriptional levels of select PS genes encoding the structural polypeptides for LH and RC complexes in Rs-fabI$_1$ using transcriptional fusions and measuring β-galactosidase activity. Transcriptional activities of *puf-lacZ*, *puc-lacZ*, and *puhA-lacZ* fusions in Rs-fabI$_1$ were not significantly different from control cells (Table 2). Thus, although PS complex levels were reduced in the presence of pRKfabI$_1$, PS gene expression was unchanged relative to control cells.

Overall levels of membrane fatty acids in *R. sphaeroides*

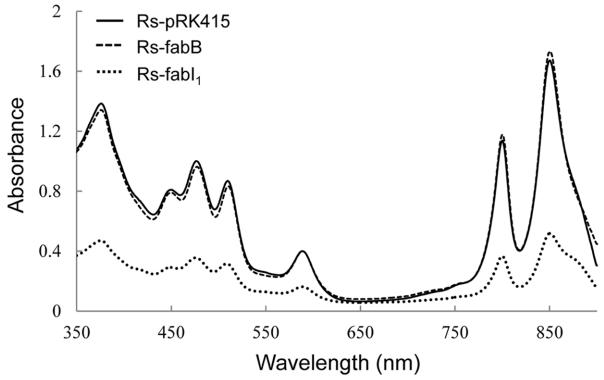

	B875 complex (nmole/mg protein)	B800-850 complex (nmole/mg protein)
Rs-pRK415	6.9 ± 0.4	23.7 ± 1.2
Rs-fabB	6.7 ± 0.5	22.9 ± 1.1
Rs-fabI$_1$	3.1 ± 0.3	6.2 ± 0.7

Fig. 2. Absorption spectra and light-harvesting complex levels of the photoheterotrophically grown Rs-fabI$_1$ and Rs-fabB.
Absorption spectra (Top) were examined with cell-free lysates from Rs-fabI$_1$, Rs-fabB, and Rs-pRK415 growing exponentially under photoheterotrophic conditions. The levels of B875 and B800-850 complexes (Bottom) were determined from the spectral profiles. All determinations were done with cells harvested from at least three independent cultures; spectral profiles shown were one of three representative experiments, and the average values of light-harvesting complex levels are shown with standard deviations.

Table 2. β-Galactosidase activity from transcriptional fusion constructs of select PS genes in photoheterotrophically grown Rs-fabI$_1$.

Fusion constructs	Strains	
	Rs-pRK415	Rs-fabI$_1$
puf::lacZ	542.3 ± 12.7[a]	518.9 ± 23.1
puc::lacZ	617.5 ± 21.2	584.3 ± 17.7
puhA::lacZ	313.1 ± 16.2	302.7 ± 18.9

[a]Miller units.

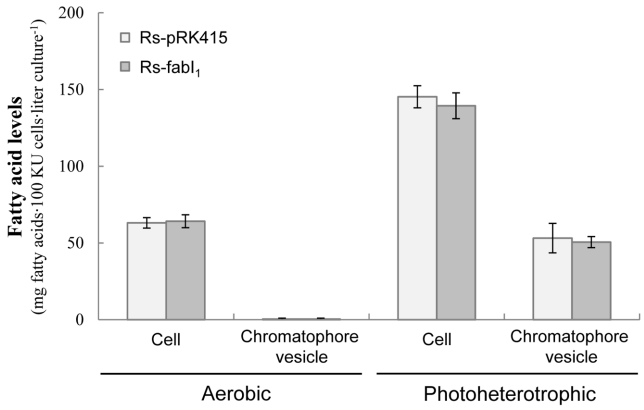

Fig. 3. Fatty acid levels of the ICM and cell membrane from aerobically and photoheterotrophically grown Rs-fabI$_1$.
Chromatophore vesicles were prepared from aerobically and photoheterotrophically grown Rs-fabI$_1$, and fatty acid levels of membrane lipids from chromatophore vesicle or whole cell lysates were determined. The level of chromatophore vesicle membrane, which is derived from the ICM, was normalized by comparing B875 complex levels with photoheterotrophically grown cells. Rs-pRK415 was included as a control. All determinations were done with cells harvested from at least three independent cultures, and average values are shown with SD.

grown under photoheterotrophic conditions were over two times more abundant than in cells grown under aerobic conditions (Fig. 3), which can be attributed to the abundance of ICM in photoheterotrophically grown cells. We then measured levels of chromatophore vesicles in Rs-fabI$_1$ grown photoheterotrophically (Fig. 3). Because chromatophore vesicles are derived from the ICM where the PS spectral complexes are exclusively localized, the levels of chromatophore vesicles reflect the overall cellular ICM levels. Cellular ICM levels were normalized by comparing the B875 complex of the chromatophore vesicles with that of the photoheterotrophically grown cells. The ICM level of Rs-fabI$_1$ (expressed in mg fatty acid of chromatophore vesicles/100 KU cells/liter culture) was not different from that of the control cells (Fig. 3). Therefore, the presence of pRKfabI$_1$ does not appear to affect ICM formation.

The Ratio of UFA to SFA in Chromatophore Vesicles from Rs-fabI$_1$ was Similarly Decreased by Half.

In order to examine the fatty acid composition of chromatophore vesicles, membrane phospholipids were extracted from chromatophore vesicles that were prepared from photoheterotrophically grown Rs-fabI$_1$ or control cells (Table 3). The fatty acid composition of chromatophore vesicles (Table 3) was similar to the cell membrane (Table 1), suggesting no difference in fatty acid composition between the ICM and plasma membrane. Notably, the ratio of UFA to SFA in chromatophore vesicles from Rs-fabI$_1$ was also decreased by half.

The major phospholipids of *R. sphaeroides* are cardiolipin (CL), phosphatidylglycerol (PG), phosphatidylcholine (PC), phosphatidylethanolamine (PE), and sulfoquinovosyl diacylglycerol (SQDG). In Rs-fabI$_1$, the cellular quantity of PC decreased to less than half that of control cells under both aerobic and photoheterotrophic conditions (Fig. 4), while PE increased under these conditions. However, the combined mole % for both PC and PE was held at constant levels. PC is synthesized from PE by PE *N*-methyltransferase (PmtA) through the methylation pathway, where PE is sequentially methylated three times using a methyl donor, S-adenosylmethionine [4]. We previously showed that the aerobic and photoheterotrophic growth of *R. sphaeroides* were not affected by disruptive mutation in *pmtA* [29].

Table 3. Fatty acid composition of membrane lipids of chromatophore vesicles prepared from photoheterotrophically grown Rs-fabI$_1$.

Strains	Composition of fatty acids (mole %)					UFA/SFA[a]
	C16	C16:1(Δ^9)	C18	C18:1(Δ^{11})	C19[b]	
Rs-pRK415	8.0 ± 0.7	1.5 ± 0.2	13.8 ± 0.9	74.4 ± 1.0	2.4 ± 0.3	3.59
Rs-fabI$_1$	15.5 ± 0.2	0.8 ± 0.1	21.7 ± 0.5	60.0 ± 1.3	2.0 ± 0.4	1.69

[a]The molar ratio of UFAs (C16:1(Δ^9), C18:1(Δ^{11}), and C19) to SFAs (C16 and C18).

[b]*cis*-11,12-Methyleneoctadecanoic acid.

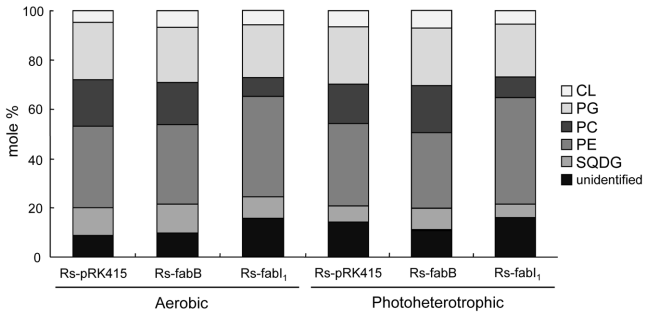

Fig. 4. Lipid composition of Rs-fabI$_1$ and Rs-fabB.

The lipid composition was determined for Rs-fabI$_1$, Rs-fabB, and Rs-pRK415. Cells were grown under aerobic and photoheterotrophic conditions. Cardiolipin (CL), phosphatidylglycerol (PG), phosphatidylcholine (PC), phosphatidylethanolamine (PE), and sulfoquinovosyl diacylglycerol (SQDG) were found in the membrane of *R. sphaeroides*. Each lipid was measured as the mole % of the total. All determinations were done with cells harvested from at least three independent cultures, and average values are shown.

Accordingly, the growth retardation of Rs-fabI$_1$ under these conditions was not attributed to the change in relative levels of PC and PE. PG was found to stimulate PmtA activity [2], but no decrease in PG was observed in Rs-fabI$_1$ (Fig. 4). It remains to be determined whether PmtA activity is affected by the increase in SFA levels in the presence of pRKfabI$_1$.

The Growth of Rs-fabI$_1$ was Restored to Wild-Type Level by the Treatment of Diazaborine or Exogenous UFA.

The enoyl-ACP reductase activity of *R. sphaeroides* grown under aerobic conditions (Fig. 5A) was approximately 7-fold lower than cells grown under photoheterotrophic conditions (Fig. 5B). The higher activity under photoheterotrophic conditions is likely due to the higher fatty acid synthesis needed for the formation of the ICM. The enoyl-ACP reductase activity of Rs-fabI$_1$ under aerobic and photoheterotrophic conditions was elevated approximately 3- to 4-fold compared with control cells (Fig. 5). Diazaborine is a specific inhibitor of enoyl-ACP reductase [5, 7, 32]. Diazaborine-treated cultures of Rs-fabI$_1$ displayed lower enoyl-ACP reductase activity in a dose-dependent way (Figs. 5A and 5B). Additionally, diazaborine treatment of Rs-fabI$_1$ resulted in a dose-dependent restoration of overall fatty acid composition, similar to control cells (Fig. 6), as well as a restoration of wild-type growth rates (Fig. S1). Lastly, LH complex levels were also restored to control levels in the presence of diazaborine (Table 4).

Because levels of the unsaturated *cis*-vaccenic (C18:1(Δ^{11})) and palmitoleic (C16:1(Δ^{9})) acids were reduced in Rs-fabI$_1$

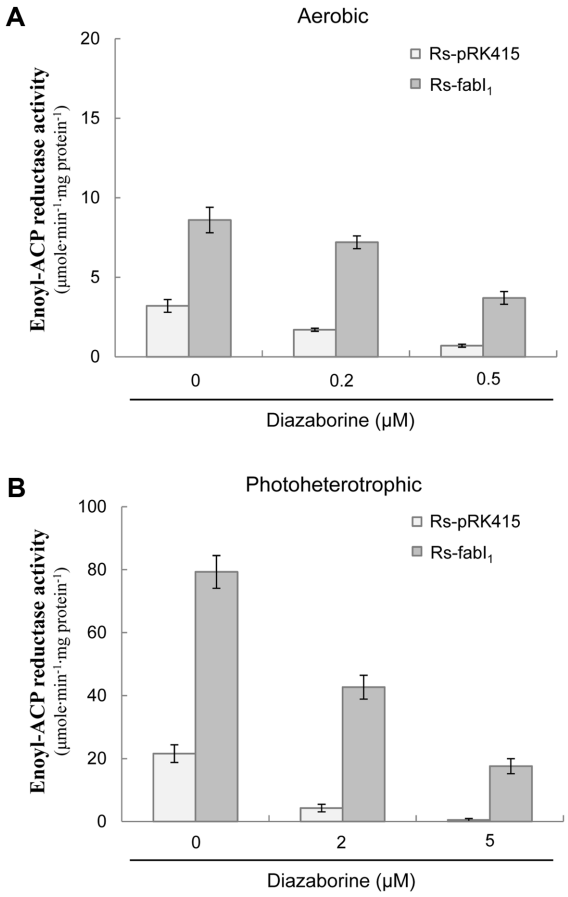

Fig. 5. Enoyl-ACP reductase activities of aerobically and photoheterotrophically grown Rs-fabI$_1$ in the presence of diazaborine.

Rs-fabI$_1$ was grown aerobically (**A**) and photoheterotrophically (**B**) in the presence of varying concentrations of diazaborine. The enoyl-ACP reductase activity of the exponentially growing cells was determined. Rs-pRK415 was included as a control. All determinations were done with cells harvested from at least three independent cultures, and the average values are shown with SD.

(Table 1), we examined whether the attenuated photoheterotrophic growth phenotype could be complemented by the exogenous addition of these two UFAs. The exogenous addition of *cis*-vaccenic acid (0.003% (w/v)) resulted in an increase of this fatty acid within the membrane of Rs-fabI$_1$ (Fig. 7) nearly to that of the control cells (Table 1), whereas the exogenous addition of palmitoleic acid (0.003% (w/v)) resulted in an increase of this fatty acid up to approximately 16 mole % (Fig. 7). The relative levels of the SFAs, palmitate (C16) and stearate (C18), of Rs-fabI$_1$ were also restored to that of control cells (Table 1) under these conditions (Fig. 7). Thus, the ratio of UFA to SFA of Rs-fabI$_1$ was restored to approximately 4 (~80% UFA) (Fig. 7), and these cells grew

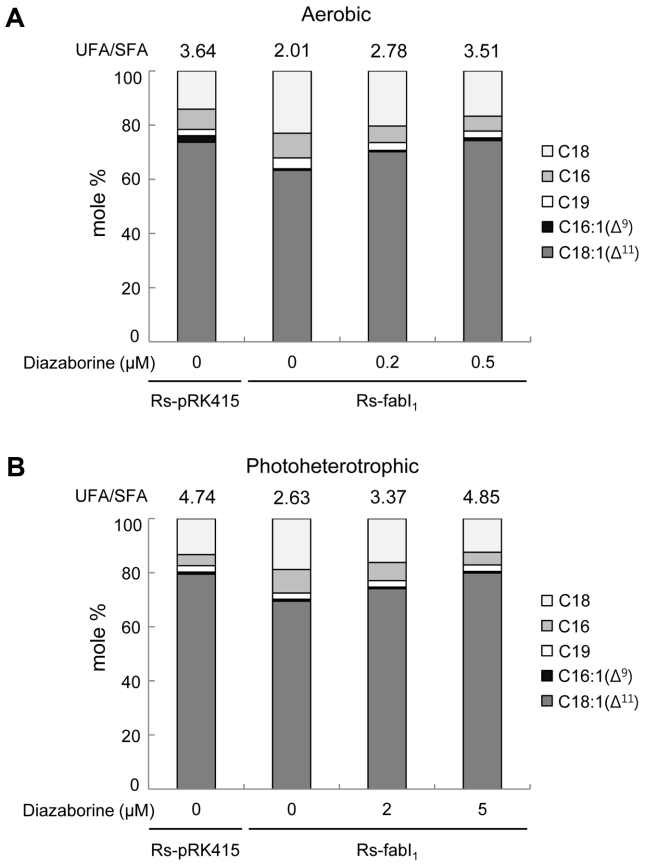

Fig. 6. Effect of diazaborine on the fatty acid composition of aerobically and photoheterotrophically grown Rs-fabI$_1$.

Rs-fabI$_1$ was grown aerobically (**A**) and photoheterotrophically (**B**) in the presence of varying concentrations of diazaborine, and the fatty acid composition of membrane lipids of exponentially growing cells was determined. Rs-pRK415 was included as a control. All determinations were done with cells harvested from at least three independent cultures, and the average values are shown. The UFA to SFA ratio is shown above each bar.

Table 4. LH complex levels of Rs-fabI$_1$ grown in the presence of diazaborine under photoheterotrophic conditions.

Diazaborine (μM)	B875 complex		B800-850 complex	
	Rs-pRK415	Rs-fabI$_1$	Rs-pRK415	Rs-fabI$_1$
0	6.9 ± 0.4[a]	3.1 ± 0.3	23.7 ± 1.2	6.2 ± 0.7
2	2.1 ± 0.1	3.9 ± 0.2	10.2 ± 1.9	17.9 ± 1.9
5	ND[b]	6.3 ± 0.3	ND	24.5 ± 2.1

[a]nmol/mg protein.

[b]Not determined.

at rates similar to control cells (Fig. S2). Lastly, LH complex levels were also restored to wild-type levels with exogenous UFA treatment (Table 5).

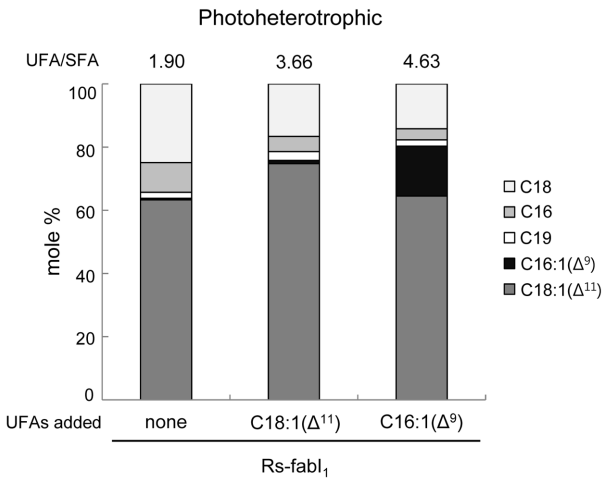

Fig. 7. Effect of exogenous *cis*-vaccenic acid and palmitoleic acid on the fatty acid composition of photoheterotrophically grown Rs-fabI$_1$.

Rs-fabI$_1$ was grown photoheterotrophically in the presence of exogenous *cis*-vaccenic acid (C18:1(Δ^{11}) or palmitoleic acid (C16:1(Δ^9)). Each UFA was used at 0.003%. The fatty acid composition of membrane lipids from exponentially growing cells was determined. All determinations were done with cells harvested from at least three independent cultures, and the average values are shown. The UFA to SFA ratio is shown above each bar.

Table 5. LH complex levels of Rs-fabI$_1$ grown in the presence of exogenous *cis*-vaccenic acid and palmitoleic acid under photoheterotrophic conditions.

UFA[a] added	B875 complex		B800-850 complex	
	Rs-pRK415	Rs-fabI$_1$	Rs-pRK415	Rs-fabI$_1$
None	7.1 ± 0.3[b]	3.4 ± 0.1	23.2 ± 1.0	7.3 ± 0.3
C18:1(Δ^{11})[c]	7.0 ± 0.4	6.8 ± 0.4	23.0 ± 1.4	22.2 ± 1.4
C16:1(Δ^9)[c]	6.7 ± 0.4	5.9 ± 0.3	22.3 ± 1.3	21.0 ± 1.2

[a]Fatty acids were dissolved in Brij 58 (0.4%) before the exogenous addition to the culture.

[b]nmol/mg protein.

[c]Each UFA was added at 0.003%.

Membrane Fluidity of Rs-fabB was Unchanged Compared with Control Cells, but That of Rs-fabI$_1$ was Significantly Decreased.

The fluorescence polarization method, using DPH as a molecular probe, has been widely applied to determine biological membrane fluidity [42]. The fluorescence anisotropy of DPH, which is inversely proportional to membrane fluidity, was measured in photoheterotrophically grown Rs-fabI$_1$ and Rs-fabB at three different temperatures. The fluorescence anisotropy in Rs-fabB was unchanged

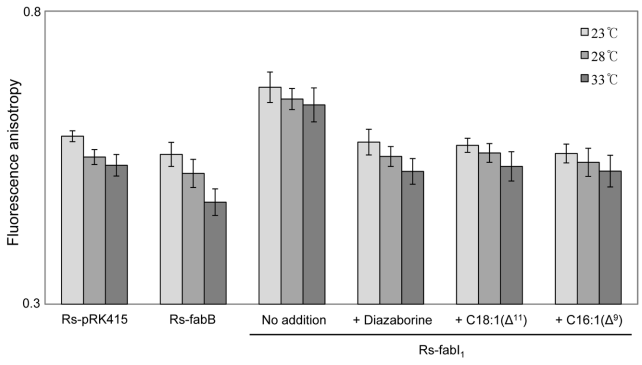

Fig. 8. Fluorescence anisotropy of Rs-fabI$_1$.

The fluorescence anisotropy of *R. sphaeroides* membranes was determined using DPH at three different temperatures (23°C, 28°C, and 33°C). Rs-fabI$_1$, Rs-fabB, and Rs-pRK415 were grown under photoheterotrophic conditions. The anisotropy was also measured with Rs-fabI$_1$ grown in the presence of either diazaborine (5 μM), or the exogenous UFA (0003%) *cis*-vaccenic acid (C18:1(Δ^{11})) or palmitoleic acid (C16:1(Δ^{9})). All determinations were done with cells harvested from at least three independent cultures, and the average values are shown with SD.

relative to control cells grown at 23°C and 28°C, but was decreased at 33°C (Fig. 8), which is reflective of a high UFA to SFA ratio (Table 1). Thus, the membrane fluidity of Rs-fabB is similar to that of control cells at ambient temperatures, even though these cells have a higher membrane UFA content of ~90%.

The fluorescence anisotropy in Rs-fabI$_1$ was almost 20–30% higher than that of control cells at all temperatures (Fig. 8), suggesting that membrane fluidity decreased due to the increase in SFA levels. However, membrane fluidity was restored to that of the control cells with diazaborine treatment (5 μM) (Fig. 8). When diazaborine was added at levels less than 5 μM, membrane fluidity was only partially restored, with UFA to SFA ratios between 2 (65% UFA) and 4 (80% UFA) (data not shown). Membrane fluidity was also restored by the exogenous addition (0.003% (w/v)) of either *cis*-vaccenic acid or palmitoleic acid to the cell cultures (Fig. 8).

In summary, the normal ratio of cellular UFA to SFA of *R. sphaeroides* is approximately 4 (~80% UFA), but decreased to 2 (~65% UFA) when enoyl-ACP reductase activity was elevated, resulting in lower membrane fluidity. However, the UFA to SFA ratio was restored to 4 either by the addition of diazaborine or by exogenous UFA. The ratio of UFA to SFA was changed to approximately 9 (~90% UFA) by elevating the dosage of *fabB* coding for β-ketoacyl-ACP synthase I, but this did not result in a change in membrane fluidity. Thus, the membrane fluidity of *R. sphaeroides* remains unchanged when UFA levels stay between 80% and 90%, and fluidity appears to be largely affected when UFA levels are lower than 80%.

Discussion

In this work, we examined the effects of changing the cellular ratio of UFA to SFA in *R. sphaeroides* by overexpressing several key fatty acid biosynthetic enzymes. We found when the ratio of UFA to SFA was increased from approximately 4 (~80% UFA) to 9 (~90% UFA) in Rs-fabB, membrane fluidity was not affected. However, membrane fluidity was decreased when the UFA to SFA ratio was lowered to 2 (~65% UFA) in Rs-fabI$_1$. The levels of LH complexes were decreased under this condition. The decreased levels of LH complexes in photoheterotrophically grown Rs-fabI$_1$ may not be entirely due to decreased membrane fluidity, because these cells also had attenuated growth rates when grown anaerobically (with DMSO). Accordingly, the decrease in LH complex levels may originate from slower growth under anaerobic (with DMSO) conditions. However, it still remains to be determined whether the assembly of LH complexes is affected when UFA levels decrease to ~65% in the presence of pRKfabI$_1$.

As far as we know, the fatty acid desaturase, which generates unsaturated fatty acids by introducing a double bond into pre-existing saturated fatty acids [1, 10, 41, 48, 56], is not present in *R. sphaeroides*. Similar to *E. coli*, the only way to synthesize unsaturated fatty acids is by the insertion of double bonds during *de novo* biosynthesis of fatty acids. A *trans*-2 form of decenoyl-ACP, instead of being reduced by FabI, may be isomerized to its *cis*-3 isomer by FabA. If the subsequent elongation of *cis*-Δ^3-decenoyl-ACP, which is metabolized through condensation with a malonyl moiety by FabB, is repeated four more times, *cis*-vaccenic acid is formed [9, 44]. Thus, *trans*-Δ^2-decenoyl-ACP is the substrate shared by FabI and FabA. If FabI is overexpressed, *trans*-Δ^2-decenoyl-ACP is reduced using NADPH to form the saturated fatty acyl-ACP. We showed that the increase in gene dosage of *fabA* did not alter the UFA to SFA ratio of *R. sphaeroides* (data not shown but similar to that observed with the control cells of Table 1). Accordingly, the equilibrium constant for the FabA-mediated isomerization of *trans*-Δ^2-decenoyl-ACP of *R. sphaeroides* is thought to be close to 1. Rather, the UFA to SFA ratio of *R. sphaeroides* is elevated to 9 by the expression of pRKfabB. Thus, the increased condensation of the *cis*-Δ^3-decenoyl moiety with malonyl-ACP by FabB appears to drive the metabolic flux to the formation of UFA.

The lowered ratio of UFA to SFA in Rs-fabI$_1$ was restored to wild-type levels by the exogenous addition of *cis*-vaccenic acid or palmitoleic acid. In the presence of the exogenous palmitoleic acid, Rs-fabI$_1$ showed a 10-fold higher occurrence of palmitoleic acid in the membrane compared with control cells (Fig. 7). Thus, exogenously added UFA appears to influence the intracellular pool of UFA and SFA, which in turn may determine the differential synthesis of UFA and SFA in *R. sphaeroides*. It remains to be determined how the UFA to SFA ratio of *R. sphaeroides* is regulated through fatty acid biosynthesis in response to exogenous fatty acids.

In summary, the membrane fluidity of *R. sphaeroides* decreases considerably when the UFA content of membrane lipids is approximately 65%, and this cellular change affects growth rates under several growth conditions. However, membrane fluidity and cell growth remain unchanged when UFA levels stay in a range of approximately 80% to 90%. These results highlight the importance of bacterial regulation of membrane fatty acid composition in *R. sphaeroides*, which is capable of growing in a wide range of growth conditions under a variety of metabolic strategies.

Acknowledgments

This work was supported by the Pioneer Research Center Program through the NRF (No. 2013M3C1A3064325) as well as by the Mid-Career Researcher Program through the NRF (No. 2009-0092822). This work was also supported by the Basic Science Research Program through the NRF (Nos. 2009-0093822 and 2012R1A1A2007943) as well as by the Intelligent Synthetic Biology Center of Global Frontier Project (No. 2013M3A6A8073562) funded by the Ministry of Science, ICT & Future Planning.

References

1. Aguilar PS, de Mendoza D. 2006. Control of fatty acid desaturation: a mechanism conserved from bacteria to humans. *Mol. Microbiol.* **62:** 1507-1514.
2. Aktas M, Narberhaus FJ. 2009. *In vitro* characterization of the enzyme properties of the phospholipid *N*-methyltransferase PmtA from *Agrobacterium tumefaciens*. *J. Bacteriol.* **191:** 2033-2041.
3. Aricha B, Fishov I, Cohen Z, Sikron N, Pesakhov S, Khozin-Goldberg I, *et al*. 2004. Differences in membrane fluidity and fatty acid composition between phenotypic variants of *Streptococcus pneumoniae*. *J. Bacteriol.* **186:** 4638-4644.
4. Arondel V, Benning C, Somerville CR. 1993. Isolation and functional expression in *Escherichia coli* of a gene encoding phosphatidylethanolamine methyltransferase (EC 2.1.1.17) from *Rhodobacter sphaeroides*. *J. Biol. Chem.* **268:** 16002-16008.
5. Baldock C, Rafferty JB, Sedelnikova SE, Baker PJ, Stuitje AR, Slabas AR, *et al*. 1996. A mechanism of drug action revealed by structural studies of enoyl reductase. *Science* **274:** 2107-2110.
6. Benning C, Somerville CR. 1992. Isolation and genetic complementation of a sulfolipid-deficient mutant of *Rhodobacter sphaeroides*. *J. Bacteriol.* **174:** 2352-2360.
7. Bergler H, Wallner P, Ebeling A, Leitinger B, Fuchsbichler S, Aschauer H, *et al*. 1994. Protein EnvM is the NADH-dependent enoyl-ACP reductase (FabI) of *Escherichia coli*. *J. Biol. Chem.* **269:** 5493-5496.
8. Camara-Artigas A, Brune D, Allen JP. 2002. Interactions between lipids and bacterial reaction centers determined by protein crystallography. *Proc. Natl. Acad. Sci. USA* **99:** 11055-11060.
9. Cronan JE. 2006. A bacterium that has three pathways to regulate membrane lipid fluidity. *Mol. Microbiol.* **60:** 256-259.
10. Cybulski LE, Albanesi D, Mansilla MC, Altabe S, Aguilar PS, de Mendoza D. 2002. Mechanism of membrane fluidity optimization: isothermal control of the *Bacillus subtilis* acyl-lipid desaturase. *Mol. Microbiol.* **45:** 1379-1388.
11. Davis J, Donohue TJ, Kaplan S. 1988. Construction, characterization, and complementation of a Puf-mutant of *Rhodobacter sphaeroides*. *J. Bacteriol.* **170:** 320-329.
12. de Mendoza D, Klages UA, Cronan JE Jr. 1983. Thermal regulation of membrane fluidity in *Escherichia coli*. Effects of overproduction of beta-ketoacyl-acyl carrier protein synthase I. *J. Biol. Chem.* **258:** 2098-2101.
13. Dezi M, Francia F, Mallardi A, Colafemmina G, Palazzo G, Venturoli G. 2007. Stabilization of charge separation and cardiolipin confinement in antenna-reaction center complexes purified from *Rhodobacter sphaeroides*. *Biochim. Biophys. Acta* **1767:** 1041-1056.
14. Dickson L, Bull ID, Gates PJ, Evershed RP. 2009. A simple modification of a silicic acid lipid fractionation protocol to eliminate free fatty acids from glycolipid and phospholipid fractions. *J. Microbiol. Methods* **78:** 249-254.
15. Donohue TJ, McEwan AG, Kaplan S. 1986. Cloning, DNA sequence, and expression of the *Rhodobacter sphaeroides* cytochrome *c*2 gene. *J. Bacteriol.* **168:** 962-972.
16. Dryden SC, Kaplan S. 1990. Localization and structural analysis of the ribosomal RNA operons of *Rhodobacter sphaeroides*. *Nucleic Acids Res.* **18:** 7267-7277.
17. Ellmann GL. 1959. Tissue sulfhydryl groups. *Anal. Biochem.* **82:** 70-77.
18. Feng Y, Cronan JE. 2009. *Escherichia coli* unsaturated fatty acid synthesis: complex transcription of the *fabA* gene and *in vivo* identification of the essential reaction catalyzed by FabB. *J. Biol. Chem.* **284:** 29526-29535.
19. Garwin JL, Klages AL, Cronan JE Jr. 1980. Beta-ketoacyl-acyl carrier protein synthase II of *Escherichia coli*. Evidence for function in the thermal regulation of fatty acid synthesis. *J. Biol. Chem.* **255:** 3263-3265.
20. Gomelsky M, Kaplan S. 1995. Genetic evidence that PpsR

from *Rhodobacter sphaeroides* 2.4.1 functions as a repressor of *puc* and *bchF* expression. *J. Bacteriol.* **177:** 1634-1637.
21. Heath RJ, Rock CO. 1995. Enoyl-acyl carrier protein reductase (FabI) plays a determinant role in completing cycles of fatty acid elongation in *Escherichia coli*. *J. Biol. Chem.* **270:** 26538-26542.
22. Heath RJ, Su N, Murphy CK, Rock CO. 2000. The enoyl-(acylcarrier-protein) reductases FabI and FabL from *Bacillus subtilis*. *J. Biol. Chem.* **275:** 40128-40133.
23. Hirano M, Satoh K, Katoh S. 1981. The effect on photosynthetic electron transport of temperature-dependent changes in the fluidity of the thylakoid membrane in a thermophilic blue-green alga. *Biochim. Biophys. Acta* **635:** 476-487.
24. Hoang TT, Schweizer HP. 1999. Characterization of *Pseudomonas aeruginosa* enoyl-acyl carrier protein reductase (FabI): a target for the antimicrobial triclosan and its role in acylated homoserine lactone synthesis. *J. Bacteriol.* **181:** 5489-5497.
25. Jackowski S, Murphy CM, Cronan JE Jr, Rock CO. 1991. Acetoacetyl-acyl carrier protein synthase. A target for the antibiotic thiolactomycin. *J. Biol. Chem.* **264:** 7624-7629.
26. Jones MR. 2007. Lipids in photosynthetic reaction centres: structural roles and functional holes. *Prog. Lipid Res.* **46:** 56-87.
27. Keen NT, Tamaki S, Kobayashi D, Trollinger D. 1998. Improved broad-host-range plasmids for DNA cloning in gram-negative bacteria. *Gene* **70:** 191-197.
28. Kho DH, Yoo SB, Kim JS, Kim EJ, Lee JK. 2004. Characterization of Cu- and Zn-containing superoxide dismutase of *Rhodobacter sphaeroides*. *FEMS Microbiol. Lett.* **234:** 261-267.
29. Kim EJ, Kim MS, Lee JK. 2007. Phosphatidylcholine is required for the efficient formation of photosynthetic membrane and B800-850 light-harvesting complex in *Rhodobacter sphaeroides*. *J. Microbiol. Biotechnol.* **17:** 373-377.
30. Lee IH, Kim EJ, Cho YH, Lee JK. 2002. Characterization of a novel enoyl-acyl carrier protein reductase of diazaborine-resistant *Rhodobacter sphaeroides* mutant. *Biochem. Biophys. Res. Commun.* **299:** 621-627.
31. Lee JK, Kaplan S. 1992. *Cis*-acting regulatory elements involved in oxygen and light control of *puc* operon transcription in *Rhodobacter sphaeroides*. *J. Bacteriol.* **174:** 1146-1157.
32. Levy CW, Baldock C, Wallace AJ, Sedelnikova S, Viner RC, Clough JM, *et al*. 2001. A study of the structure-activity relationship for diazaborine inhibition of *Escherichia coli* enoyl-ACP reductase. *J. Mol. Biol.* **309:** 171-180.
33. Los DA, Mironov KS, Allakhverdiev SI. 2013. Regulatory role of membrane fluidity in gene expression and physiological functions. *Photosynth. Res.* **116:** 489-509.
34. Mackenzie C, Eraso JM, Choudhary M, Roh JH, Zeng X, Bruscella P, *et al*. 2007. Postgenomic adventures with *Rhodobacter sphaeroides*. *Annu. Rev. Microbiol.* **61:** 283-307.
35. Markwell MA, Haas SM, Bieber LL, Tolbert NE. 1978. A modification of the Lowry procedure to simplify protein determination in membrane and lipoprotein samples. *Anal. Biochem.* **87:** 206-210.
36. Marr AG, Ingraham JL. 1962. Effect of temperature on the composition of fatty acids in *Escherichia coli*. *J. Bacteriol.* **84:** 1260-1267.
37. Marrakchi H, Choi KH, Rock CO. 2002. A new mechanism for anaerobic unsaturated fatty acid formation in *Streptococcus pneumoniae*. *J. Biol. Chem.* **277:** 44809-44816.
38. Massengo-Tiassé RP, Cronan JE. 2009. Diversity in enoyl-acyl carrier protein reductases. *Cell. Mol. Life Sci.* **66:** 1507-1517.
39. Meinhardt SW, Kiley PJ, Kaplan S, Crofts AR, Harayama S. 1985. Characterization of light-harvesting mutants of *Rhodopseudomonas sphaeroides*. I. Measurement of the efficiency of energy transfer from light-harvesting complexes to the reaction center. *Arch. Biochem. Biophys.* **236:** 130-139.
40. Mikami K, Murata N. 2003. Membrane fluidity and the perception of environmental signals in cyanobacteria and plants. *Prog. Lipid Res.* **42:** 527-543.
41. Murata N, Wada H. 1995. Acyl-lipid desaturases and their importance in the tolerance and acclimatization to cold of cyanobacteria. *Biochem. J.* **308:** 1-8.
42. Mykytczuk NC, Trevors JT, Leduc LG, Ferroni GD. 2007. Fluorescence polarization in studies of bacterial cytoplasmic membrane fluidity under environmental stress. *Prog. Biophys. Mol. Biol.* **95:** 60-82.
43. Oh JI, Kaplan S. 2001. Generalized approach to the regulation and integration of gene expression. *Mol. Microbiol.* **39:** 1116-1123.
44. Parsons JB, Rock CO. 2013. Bacterial lipids: metabolism and membrane homeostasis. *Prog. Lipid Res.* **52:** 249-276.
45. Quémard A, Sacchettini JC, Dessen A, Vilcheze C, Bittman R, Jacobs WR Jr, Blanchard JS. 1995. Enzymatic characterization of the target for isoniazid in *Mycobacterium tuberculosis*. *Biochemistry* **34:** 8235-8241.
46. Sakamoto T, Los DA, Higashi S, Wada H, Nishida I, Ohmori M, Murata N. 1994. Cloning of omega 3 desaturase from cyanobacteria and its use in altering the degree of membrane-lipid unsaturation. *Plant Mol. Biol.* **26:** 249-263.
47. Schägger H, von Jagow G. 1987. Tricine-sodium dodecyl sulfate-polyacrylamide gel electrophoresis for the separation of proteins in the range from 1 to 100 kDa. *Anal. Biochem.* **166:** 368-379.
48. Shanklin J, Somerville C. 1991. Stearoyl-acyl-carrier-protein desaturase from higher plants is structurally unrelated to the animal and fungal homologs. *Proc. Natl. Acad. Sci. USA* **88:** 2510-2514.
49. Simkiss K. 1998. Cell membranes; barriers, regulators and transducers? *Comp. Biochem. Physiol. A Mol. Integr. Physiol.* **120:** 17-22.
50. Simons RW, Houman F, Kleckner N. 1987. Improved single and multicopy *lac*-based cloning vectors for protein and operon fusions. *Gene* **53:** 85-96.
51. Sistrom WR. 1962. The kinetics of the synthesis of photopigments in *Rhodopseudomonas sphaeroides*. *J. Gen. Microbiol.* **28:** 607-616.
52. Tai TN, Havelka WA, Kaplan S. 1988. A broad host-range

vector system for cloning and translational *lacZ* fusion analysis. *Plasmid* **19:** 175-188.
53. Tehrani A, Prince RC, Beatty TJ. 2003. Effects of photosynthetic reaction center H protein domain mutations on photosynthetic properties and reaction center assembly in *Rhodobacter sphaeroides*. *Biochemistry* **42:** 8919-8928.
54. Tucker JD, Siebert CA, Escalante M, Adams PG, Olsen JD, Otto C, *et al*. 2010. Membrane invagination in *Rhodobacter sphaeroides* is initiated at curved regions of the cytoplasmic membrane, then forms both budded and fully detached spherical vesicles. *Mol. Microbiol.* **76:** 833-847.
55. White SW, Zheng J, Zhang YM, Rock CO. 2005. The structural biology of type II fatty acid biosynthesis. *Annu. Rev. Biochem.* **74:** 791-831.
56. Zhu K, Choi KH, Schweizer HP, Rock CO, Zhang YM. 2006. Two aerobic pathways for the formation of unsaturated fatty acids in *Pseudomonas aeruginosa*. *Mol. Microbiol.* **60:** 260-273.